Original Article

Evaluation of Dose Distribution and Normal Tissue Complication Probability of a Combined Dose of Cone-Beam Computed Tomography Imaging with Treatment in Prostate Intensity-Modulated Radiation Therapy

Tetsuya Tomita[1,2], Tomonori Isobe[3], Yoshinobu Furuyama[4], Hideyuki Takei[3], Daisuke Kobayashi[1,2], Yutaro Mori[3], Toshiyuki Terunuma[3], Eisuke Sato[5], Hiroshi Yokota[2], Takeji Sakae[3]

[1]Graduate School of Comprehensive Human Sciences, University of Tsukuba, Ibaraki, [2]Department of Radiology, University of Tsukuba Hospital, Ibaraki, [3]Faculty of Medicine, University of Tsukuba, Ibaraki, [4]Department of Radiology, Chiba University Hospital, Chiba, [5]Faculty of Health Sciences, Juntendo University, Tokyo, Japan

Abstract

Purpose: The purpose of this study is to evaluate the effects of cone-beam computed tomography (CBCT) on dose distribution and normal tissue complication probability (NTCP) by constructing a comprehensive dose evaluation system for prostate intensity-modulated radiation therapy (IMRT). **Methods:** A system that could combine CBCT and treatment doses with MATLAB was constructed. Twenty patients treated with prostate IMRT were studied. A mean dose of 78 Gy was prescribed to the prostate region, excluding the rectal volume from the target volume, with margins of 4 mm to the dorsal side of the prostate and 7 mm to the entire circumference. CBCT and treatment doses were combined, and the dose distribution and the NTCP of the rectum and bladder were evaluated. **Results:** The radiation dose delivered to 2% and 98% of the target volume increased by 0.90 and 0.74 Gy on average, respectively, in the half-fan mode and on average 0.76 and 0.72 Gy, respectively, in the full-fan mode. The homogeneity index remained constant. The percent volume of the rectum and bladder irradiated at each dose increased slightly, with a maximum increase of <1%. The rectal NTCP increased by approximately 0.07% from 0.46% to 0.53% with the addition of a CBCT dose, while the maximum NTCP in the bladder was approximately 0.02%. **Conclusions:** This study demonstrated a method to evaluate a combined dose of CBCT and a treatment dose using the constructed system. The combined dose distribution revealed increases of <1% volume in the rectal and bladder doses and approximately 0.07% in the rectal NTCP.

Keywords: Cone-beam computed tomography, image-guided radiation therapy, imaging dose, intensity-modulated radiation therapy, normal tissue complication probability

Received on: 16-01-2020 **Review completed on:** 02-03-2020 **Accepted on:** 31-03-2020 **Published on:** 20-07-2020

Introduction

In recent years, with the advancement of radiation therapy technology, intensity-modulated radiation therapy (IMRT) has become popular. IMRT is an irradiation method that locally administers a high dose to a tumor while sparing the surrounding normal tissues. For IMRT for prostate cancer, as there are risk organs – particularly the rectum and the bladder – near the prostate, a steep dose distribution is formed at the boundary between the prostate and the risk organs. If there is any deviation from the computed tomography (CT) image in the patient setup during treatment, not only will the dose delivered to the prostate be insufficient, but also a high dose may be administered to the surrounding normal organs. Therefore, a treatment plan that considers both the patient setup during treatment and anatomical variations is important.

Access this article online

Quick Response Code:

Website: www.jmp.org.in

DOI: 10.4103/jmp.JMP_4_20

Address for correspondence: Prof. Tomonori Isobe, 1-1-1 Tennodai, Tsukuba, Ibaraki, Japan.
E-mail: tiso@md.tsukuba.ac.jp

How to cite this article: Tomita T, Isobe T, Furuyama Y, Takei H, Kobayashi D, Mori Y, *et al*. Evaluation of dose distribution and normal tissue complication probability of a combined dose of cone-beam computed tomography imaging with treatment in prostate intensity-modulated radiation therapy. J Med Phys 2020;45:78-87.

This challenge has been significantly addressed by the introduction of image-guided radiation therapy (IGRT). IGRT is a reference technology that reproduces the irradiation position determined in the treatment plan by measuring and correcting the patient position displacement during treatment. It is based on the image information obtained immediately before and during irradiation at various frequencies depending on the facility.[1-4] The images are obtained with on-board kV imagers, oblique X-ray imagers, or cone-beam computed tomography (CBCT). Therefore, IGRT involves radiation exposure, and the absorbed imaging doses measured at the skin surface have been reported as 0.2–0.6 mGy in two-directional imaging with on-board kV imagers, 0.3–0.6 mGy with oblique X-ray imagers, and 30–60 mGy with CBCT.[5-7] Even if the imaging dose is small, it cannot be ignored when a large number of fractions is required, such as the 30 or more fractions needed for IMRT for prostate cancer. Obtaining images by CBCT after 39 prostate IMRT fractions result in an approximately 1 Gy dose at the isocenter.[8] Hence, patients are exposed to a considerable CBCT imaging dose.

Ding *et al*. calculated the imaging doses of various devices used in IGRT through Monte Carlo (MC) simulations and showed the imaging dose distribution in a patient's body.[9-12] However, the total dose, including the imaging dose, was not evaluated in their study. Although some studies reported methods to combine the imaging dose with the treatment dose,[13-15] none of them have evaluated the combined dose on clinical CT images with contours using MC simulation. According to the American Association of Physicists in Medicine (AAPM) Task Group 180 Report, the imaging dose should be included in the prescription dose if the imaging dose exceeds 5% of the prescription dose.[16] However, this report did not show how to evaluate the combined dose, which is the sum of the imaging dose and the treatment dose. Furthermore, the radiation treatment planning system (RTPS) currently used in clinical practice cannot determine the imaging dose from IGRT image acquisition and thus cannot comprehensively evaluate the total dose.

Therefore, this study aims to demonstrate a method to evaluate the combined dose of CBCT imaging and the treatment dose in prostate IMRT. For this purpose, we constructed a system that can calculate the CBCT dose and add it to the treatment dose. Furthermore, this system can evaluate changes in dose distribution and normal tissue complication probability (NTCP).

Methods

Patients and treatment planning

The subjects were 20 patients who underwent prostate IMRT at the University of Tsukuba Hospital from 2015 to 2018. The treatment plan for prostate IMRT was created using Pinnacle v9.10 (Philips Medical Systems, Fitchburg, WI, USA). The clinical target volume included the whole prostate with a seminal vesicle base of approximately 1 cm, plus a 4-mm margin on the dorsal side and a 7-mm margin in all other directions as the margins of the planning target volume (PTV). The prescription dose was set such that the D_{mean} of the region, excluding the rectal volume from the PTV (PTV–rectum), was 78 Gy with ± 1% error. The dose constraints were as follows: <14%, 22%, and 34% of the rectum volume receiving more than 60 Gy (V_{60}), V_{50}, and V_{35}, respectively, and <30% and 50% of the bladder receiving V_{60} and V_{45}, respectively. This study was conducted after obtaining approval from the Clinical Research Ethics Review Committee (H29-076).

Construction of a comprehensive dose evaluation system

A system that could comprehensively evaluate the treatment dose determined using the RTPS and CBCT dose was constructed with MATLAB r2018b. Figure 1 shows an overview of the system. It can perform MC simulations with the CT images used for treatment planning and dose-volume histogram (DVH) analysis after dose summation using organ structures.

The MC code EGSnrc/BEAMnrc was used.[17-20] An on-board imager v1.6 (OBI; Varian Medical Systems, Palo Alto, CA, USA), X-ray source, inherent filter, aperture, and two types of bowtie (half-bowtie and full-bowtie) filters were simulated. A phase space file with a tube voltage of 125 kV at 50 cm from the X-ray source was created in the simulation. The geometric structure and materials of each component were simulated according to the drawings provided by Varian Medical Systems. Figure 2 shows the constructed simulation system.

To confirm the accuracy of the constructed simulation system, the calculated values of the percent depth dose (*PDD*) and off-center ratio (*OCR*) in water were compared with those measured using an ionization chamber. The simulation was performed by creating a water phantom measuring 30 cm × 30 cm × 30 cm (W × L × H) using the EGSnrc/DOSXYZnrc code.[21] The calculated voxel size was set to 1 cm × 1 cm × 0.2 cm up to a depth of 1 cm, 1 cm × 1 cm × 0.5 cm up to a depth of 2 cm, and 1 cm × 1 cm × 1 cm for deeper positions to obtain the *PDD* and 0.5 cm × 0.5 cm × 0.5 cm to obtain depths of 1 and 5 cm for the *OCR*. The simulation settings included photoelectron angular sampling, Rayleigh scattering, atomic relaxation, spin effects, and electron impact ionization. The photon and electron cutoff energies were both set to 1 keV. Measurements were performed using a Farmer-type ionization chamber TM30013 (PTW, Freiburg, Germany) in a three-dimensional water phantom, with the *PDD* up to a depth of 20 cm and *OCR* at 1 and 5 cm depths. The field size was 30.3 cm × 20.6 cm when the half-bowtie filter was installed and 27.2 cm × 18.4 cm when the full-bowtie filter was installed.

The DOSXYZnrc code was used for the simulation with CT images of the patients. The DICOM format CT volume image of each patient was imported into the MC simulation system using the CTCREATE code.[21] Each voxel in the DICOM image was converted from the CT value to a specific material such as air, lung, tissue, bone, and density, and the MC simulations were performed.

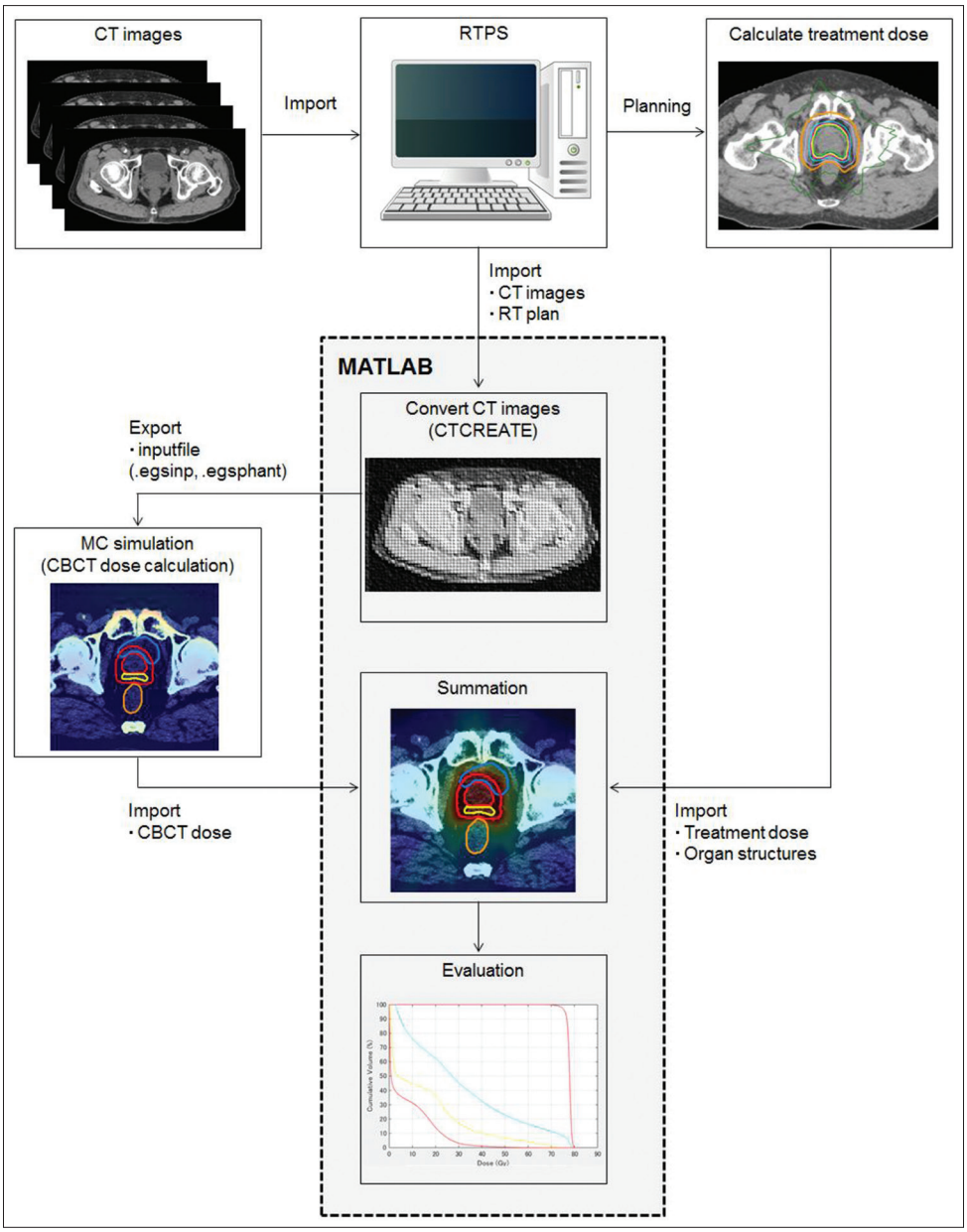

Figure 1: Schematic of our methodology. The computed tomography images used for the treatment plan and the drawn organ structure were imported into the program constructed in MATLAB. The cone-beam computed tomography dose was calculated through Monte Carlo simulation using the isocenter and treatment fractionation set in the treatment plan. Dose-volume histogram can be determined by adding the calculated cone-beam computed tomography and treatment doses calculated using the radiation treatment planning system

Monte Carlo simulation calibration

Using CT images used for treatment planning, the MC calculations were calibrated to accurately obtain the CBCT dose. The MC simulation of the CBCT dose was performed using the planning CT images of a water-equivalent polystyrene elliptical phantom (I'mRT phantom, IBA Dosimetry, Schwarzenbruck, Germany) with a detector inserted. Using the same geometry, we measured the CBCT dose using a Farmer-type ionization chamber TM30013 and converted it to the absorbed dose as follows:[22]

$$D_w = MN_k \; P_{Q,cham} \left(\frac{\overline{\mu}_{en}}{\rho} \right)^w_{air} \quad (1)$$

where D_w is the absorbed dose in water at a point in the water phantom, M is the charge with various corrections, N_k is the air kerma calibration coefficient, $P_{Q,\,cham}$ is the correction factor for the change in the chamber response, and $\left(\overline{\mu}_{en}/\rho\right)^w_{air}$ is the water-to-air ratio of the mean mass energy absorption coefficient. N_k was measured as the calibration factor from the charge of the Farmer-type ionization chamber TM30013 to the air kerma using the Accu-gold + ionization chamber (Radcal, Monrovia, CA, USA). $P_{Q,\,cham}$ and $\left(\overline{\mu}_{en}/\rho\right)^w_{air}$ were obtained from the literature.[22] Calibration was performed by comparing the measured and MC-calculated absorbed doses at the center

of the elliptical phantom, and the doses measured at eight other points were used to validate the MC calculations [Figure 3]. The calibration coefficient f_{MCcal} for converting the calculated MC value into the absorbed dose in the phantom was obtained as:

$$f_{MCcal} = \frac{D_{exp}}{D_{MCcal}} \quad (2)$$

where D_{exp} is the measured absorbed dose at the center of the elliptical phantom and D_{MCcal} is the MC-calculated value at the center of the elliptical phantom. Table 1 presents the CBCT imaging conditions for dose measurements.

Evaluation of organ dose and dose distribution

To evaluate the imaging dose for the pelvic CBCT (half-fan mode and full-fan mode), CBCT was performed 39 times. Subsequently, the doses that were delivered to 2% (D_2) and 50% (D_{50}) of volumes of the prostate, rectum, bladder, and pelvis were calculated. To compare the dose distribution of the prostate IMRT treatment plan alone and the IMRT plan combined with the CBCT dose, we analyzed the DVH of the target and risk organs. The target was evaluated using the D_2 and D_{98} of the PTV–rectum and the homogeneity index (HI), defined as $(D_2 - D_{98})/D_{50}$.[23] The risk organs were evaluated using D_2 and D_{50} of the rectum, bladder, and pelvic bones; V_{75}, V_{70}, V_{65}, and V_{60} of the rectum; and V_{80}, V_{75}, V_{70}, and V_{40} of the bladder, with and without CBCT.

Table 1: Default cone-beam computed tomography pelvic imaging conditions (pelvis and pelvis spotlight)

	Pelvis (half-fan mode)	Pelvis spotlight (full-fan mode)
Tube voltage (kV)	125	125
Tube current (mA)	80	80
Exposure time (ms)	13	25
Gantry rotation angle (°)	92-88	292-88
Exposure (mAs)	695	740
Filter	Half-bowtie	Full-bowtie

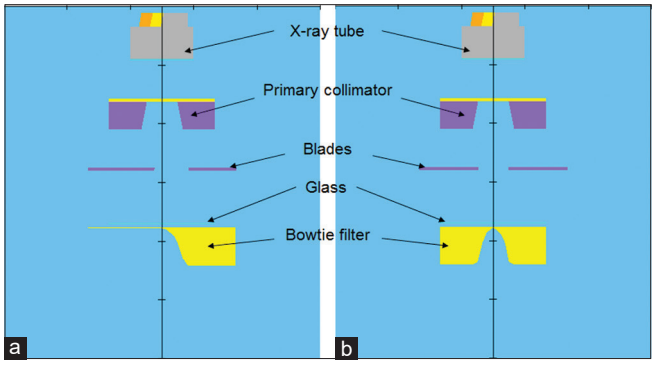

Figure 2: Schematic of the geometry of the on-board imager v1.6 device used for Monte Carlo simulation: (a) half-fan mode uses half-bowtie filter, and (b) full-fan mode uses full-bowtie filter

Normal tissue complication probability calculations for rectum and bladder

We used the formula manipulation software Mathematica 9.0 (Wolfram Research Inc., Champaign, IL, USA) and the Lyman–Kucher–Burman (LKB) model for our calculations.[24] The NTCP in the LKB model was obtained as follows.

$$NTCP = \frac{1}{\sqrt{2\pi}} \int_{-\infty}^{t} \exp\left(\frac{-t^2}{2}\right) dt \quad (3)$$

$$v = \frac{V_{eff}}{V_{ref}} \quad (4)$$

$$t = \frac{\left(D - TD_{50}(v)\right)}{\left(m \cdot TD_{50}(v)\right)} \quad (5)$$

$$TD_{50}(v) = \frac{TD_{50}(1)}{v^n} \quad (6)$$

Here, V_{eff} is the volume defined by the effective volume method;[25] if irradiated uniformly, this volume would experience a complication probability similar to that caused by the actual nonuniform dose delivered. Furthermore, V_{ref} is the total volume of the organ, n represents the volume effect dependence, and m represents the slope of the NTCP curve. Organ-specific values were obtained from the literature.[26] $TD_{50}(v)$ is a dose that causes late adverse events in 50% of patients when a partial volume of normal tissues v is uniformly irradiated, whereas TD_{50} (1) is a dose that causes late adverse events in 50% of patients when overall normal tissues are uniformly irradiated. D is the prescribed dose. There are various reports on the parameters used to calculate NTCP;[27] however, this study used the classic Burman report. The rectum was evaluated for severe proctitis, necrosis, stenosis, and fistula with $n = 0.12$, $m = 0.15$, and TD_{50} (1) = 80 Gy; the bladder was evaluated for symptomatic bladder contracture and volume loss, with $n = 0.15$, $m = 0.11$, and TD_{50} (1) = 80 Gy.[26]

Results

Consistency between simulations and actual measurements

Figure 4 shows the calculated and measured *PDD* and *OCR* with 125-kV X-rays using two types of bowtie filters. *PDD* was normalized to a depth of 10 cm. The simulation using the half-bowtie filter showed a maximum difference of 0.67% lower than the measured value up to 1.0 cm from the water surface. As the depth increased beyond 1.0 cm, the simulated value exhibited a tendency to become lower than the measured value, with a maximum difference of 3.98%. In the simulation using the full-bowtie filter, a maximum difference of 2.84% was observed from the water surface to a depth of 1.0 cm. As the depth increased, a tendency to become lower than the measured value was observed with a maximum difference between the simulated and measured value of 2.51%. The *OCR* was normalized at the center of the beam axis with a depth of 1.0 cm. The simulated *OCR* using both bowtie filters

showed disagreement with the measured *OCR* of 15.72% and 2.51%, respectively, at 1.0 cm deep, and 11.95% and 5.18%, respectively, at 5.0 cm deep inside the field. These values were 8.91% and 29.90%, respectively, at 1.0 cm deep, and 5.63% and 11.88%, respectively, at 5.0 cm deep outside the field.

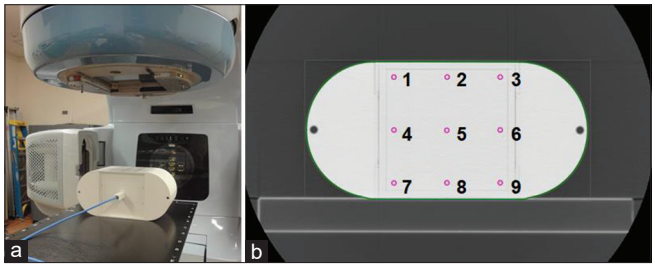

Figure 3: The cone-beam computed tomography dose was measured by inserting a Farmer-type ionization chamber TM30013 into an elliptical phantom. (a) Arrangement of phantom during cone-beam computed tomography dose measurement and (b) measurement points using the Farmer-type ionization chamber TM30013. The calculated Monte Carlo value was calibrated with the absolute dose at measurement point 5

Both bowtie filters showed relatively large errors at the edge of the field where the dose was 50% or less.

The CBCT dose in the elliptical phantom was calculated via the MC simulations for two types of imaging protocols. The calculated MC values in Table 2 were calibrated with the measured values at the center of the elliptical phantom (measurement point 5). The calculations with the half-fan mode showed a deviation of up to 5% from the actual measurements, whereas those values obtained by the full-fan mode showed a deviation of up to 8%. Calculated MC values for both types of imaging protocols tended to be higher on the ceiling side of the elliptical phantom (measurement points 1–3) and lower on the floor side (measurement points 7–9). The values at the middle section of the elliptical phantom (measurement points 4–6) tended to be lower in the half-fan mode and higher in the full-fan mode.

Organ dose and dose distribution

Figure 5 shows an example of a dose distribution map and DVH of the planned, CBCT, and combined doses. Using

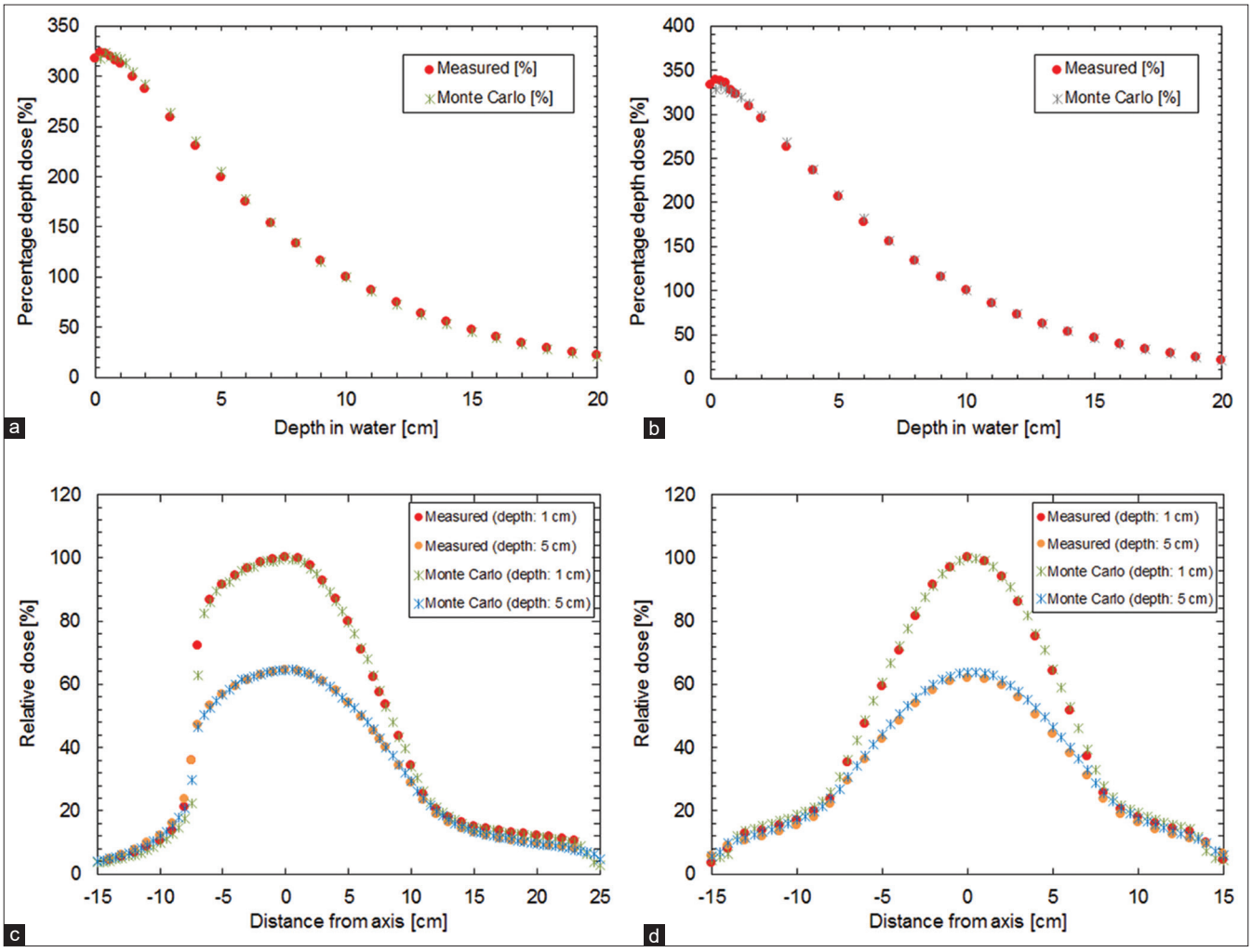

Figure 4: Comparison of 125-kV X-ray percent depth dose and off-center ratio with two bowtie filters obtained by Monte Carlo calculations and ionization chamber measurements: (a) percent depth dose (half-bowtie filter), (b) percent depth dose (full-bowtie filter), (c) off-center ratio (half-bowtie filter), and (d) off-center ratio (full-bowtie filter)

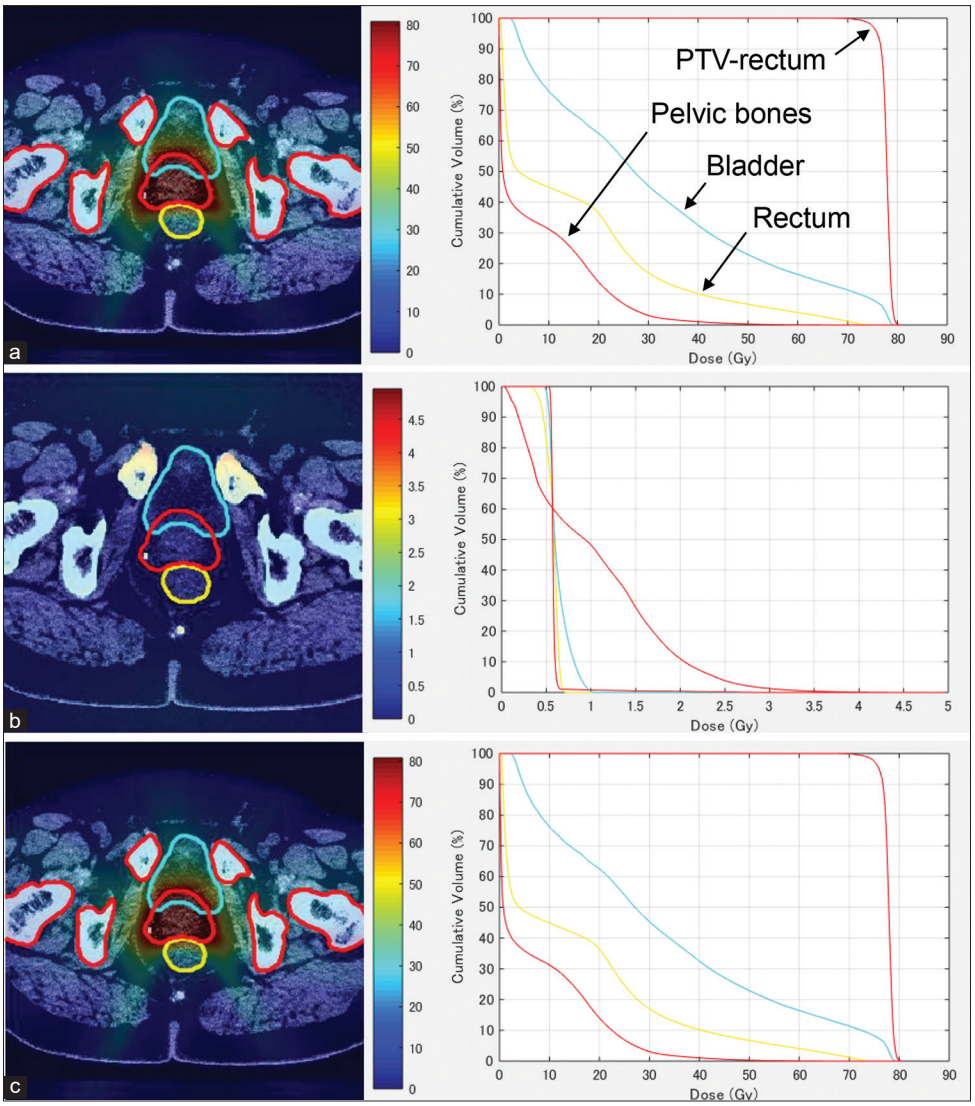

Figure 5: Calculated cone-beam computed tomography doses with the constructed system, combined with the planned treatment dose and dose–volume histogram. (a) Planned treatment dose, (b) cone-beam computed tomography dose, and (c) combined dose

Table 2: Comparison of doses obtained by Monte Carlo calculations and measured doses in an elliptical phantom

Measurement points	Pelvis (half-fan mode)			Pelvis spotlight (full-fan mode)		
	Measured (cGy)	Monte Carlo (cGy)	Difference (%)	Measured (cGy)	Monte Carlo (cGy)	Difference (%)
1	2.88	2.89	0.12	0.93	0.99	6.95
2	4.02	4.09	1.64	0.78	0.83	5.38
3	3.16	3.27	3.33	0.60	0.64	7.23
4	2.53	2.48	−1.93	2.28	2.32	1.83
5	2.67	2.67	-	2.45	2.45	-
6	2.49	2.46	−1.26	1.88	1.91	1.45
7	3.07	3.00	−2.46	4.18	4.12	−1.42
8	3.74	3.70	−1.02	5.32	5.36	0.58
9	2.78	2.66	−4.56	4.12	3.89	−5.55

The values calculated through Monte Carlo simulations were calibrated at the center of the elliptical phantom (measurement point 5)

this map, it was possible to identify only the CBCT dose, for which a dose of 3–4 Gy was observed in the pelvic bones [Figure 5b]. According to the dose distribution in the planned and combined doses, there was no significant change in both the dose distribution and/or the DVH near the prostate [Figure 5a and c].

Table 3 presents the calculation results of 39 CBCT dose fractions. D_{50} was <1 Gy in the prostate, rectum, and bladder in the half-fan mode but higher in the pelvic bones at 1.76 ± 0.27 Gy. In the full-fan mode, the average D_{50} of the prostate, bladder, and pelvic bones decreased by 17.5%, 46.6%, and 25.0%, respectively, and increased by 25.0% in the rectum, compared to the half-fan mode. In the half-fan mode, the D_2 values for the prostate, bladder, rectum, and the pelvic bones were approximately 1.3 Gy, 1.2 Gy, 0.9 Gy and 4.0 Gy, respectively. The maximum dose was around the pubic bone. In the full-fan mode, the average D_2 of the prostate and bladder decreased by 12.5% and 38.5%, respectively, compared to the half-fan mode. Conversely, the average D_2 for the rectum and pelvic bones increased by 38.7% and 10.2%, respectively, and the maximum dose was around the coccyx.

Table 4 presents the D_2, D_{98}, and HI of the target, which combines the imaging dose of 39 CBCT fractions and the treatment dose. In 39 CBCT fractions, D_2 and D_{98} increased by 0.90 Gy and 0.74 Gy, respectively, in the half-fan mode and 0.76 Gy and 0.72 Gy, respectively, in the full-fan mode. HI showed no change in either mode.

Tables 5 and 6 present the organ volume percentage for rectal and bladder doses in the combined dose DVH. For the rectum, V_{75} increased by approximately 0.1%, and V_{70}, V_{65}, and V_{60} increased by approximately 0.3%, irrespective of the imaging conditions. For the bladder, in the full-fan mode, V_{80}, V_{75}, and V_{40} increased by approximately 0.4% and V_{70} increased by 0.3%. For the bladder in the half-fan mode, both V_{80} and V_{75} increased by 0.6%, V_{70} increased by 0.4%, and V_{40} increased by 0.8%.

Normal tissue complication probability of the rectum and bladder

Table 7 presents the results of the DVH and the NTCP obtained by adding the planned and CBCT doses. Compared with the calculated planned dose, rectal NTCP increased due to the addition of the CBCT dose. The rectal NTCP increased from 0.46% to 0.53% when 39 CBCT doses were added in both the half-fan and full-fan modes. The NTCP in the urinary bladder was approximately 0.02% at most, even with the inclusion of the CBCT dose.

Discussion

Consistency between simulations and measurements

Verification of the 125-kV X-ray beam model used in the pelvic CBCT was performed using *PDD* and *OCR*. Modeling of the 125-kV X-ray beam used in the OBIs through MC simulations was reported by Ding *et al*. and Hioki *et al*.[9,28] Hioki *et al*. examined 125-kV X-rays with a half-bowtie filter similar to the filter used here and found that the difference between *PDD* and *OCR* was within 3%. The differences between the *PDD* and *OCR* obtained using the half-bowtie and the full-bowtie filters were within approximately 3% in our study as well. Hence, the model used in this study at least as accurate as Hioki *et al*.'s model.[28] However, in our study, the difference between the measured and calculated values was greater at the shallow part of the *PDD* and the irradiation field edge, where the dose at the *OCR* was <50%. The uncertainty near the surface during measurements is large, making evaluation difficult; however, the MC calculation value is considered to have a large systematic error near the surface. As the dose was low at the edge of the irradiation field, the effect on dose distribution and DVH was considered to be small.

The doses in the half-fan and full-fan modes of CBCT were simulated using the modeled beam. The calculated MC dose in the elliptical phantom differed from the dose measured by the ionization chamber up to 5% in the half-fan mode and up to 8% in the full-fan mode. Although the error was relatively large owing to the comparison of numerical values with small

Table 3: Cone-beam computed tomography doses in organs

	Mean±SD (Gy) (range)			
	Pelvis (half-fan mode)		Pelvis spotlight (full-fan mode)	
	D_2	D_{50}	D_2	D_{50}
Prostate	1.28±0.87 (0.73-3.67)	0.80±0.10 (0.55-0.99)	1.12±0.71 (0.57-3.19)	0.66±0.09 (0.47-0.77)
Rectum	0.93±0.12 (0.65-1.10)	0.84±0.11 (0.57-1.00)	1.29±0.18 (0.91-1.59)	1.05±0.16 (0.73-1.35)
Bladder	1.22±0.22 (0.75-1.61)	0.88±0.14 (0.58-1.16)	0.75±0.19 (0.29-1.13)	0.47±0.09 (0.30-0.61)
Pelvic bones	3.92±0.45 (2.70-4.65)	1.76±0.27 (0.90-2.09)	4.32±0.60 (2.83-5.16)	1.32±0.22 (0.66-1.63)

SD: Standard deviation

Table 4: D_2, D_{98}, and homogeneity index of the target

	Mean±SD (range)				
	Treatment dose	Combined dose (half-fan mode)		Combined dose (full-fan mode)	
D_2 (Gy)	79.64±0.52 (78.50-80.68)	80.54±0.50 (79.73-81.67)	P<0.001	80.40±0.51 (79.54-81.59)	P<0.001
D_{98} (Gy)	74.46±0.74 (73.06-75.67)	75.20±0.72 (73.88-76.50)	P<0.001	75.18±0.70 (73.90-76.34)	P<0.001
HI	0.07±0.01 (0.05-0.09)	0.07±0.01 (0.05-0.09)	P>0.1	0.07±0.01 (0.05-0.09)	P>0.1

For D_2, D_{98}, and HI, the significance of the difference between the two combined doses and planned treatment dose was evaluated using the Wilcoxon signed-rank test. SD: Standard deviation, HI: homogeneity index

Table 5: V_{75}, V_{70}, V_{65}, and V_{60} of the rectum

	Mean±SD (%) (range)				
	Treatment dose	Combined dose (half-fan mode)		Combined dose (full-fan mode)	
V_{75}	0.11±0.19 (0.00-0.67)	0.20±0.29 (0.01-1.04)	P<0.001	0.19±0.30 (0.01-1.10)	P<0.001
V_{70}	1.55±0.75 (0.12-2.90)	1.89±0.86 (0.16-3.31)	P<0.001	1.88±0.86 (0.18-3.32)	P<0.001
V_{65}	3.44±1.26 (0.69-5.88)	3.73±1.35 (0.78-6.38)	P<0.001	3.73±1.36 (0.78-6.40)	P<0.001
V_{60}	5.14±1.67 (1.65-8.71)	5.41±1.76 (1.75-9.22)	P<0.001	5.42±1.77 (1.78-9.25)	P<0.001

For V_{75}, V_{70}, V_{65}, and V_{60}, the significance of the difference between the two combined doses and planned treatment dose was evaluated using the Wilcoxon-signed rank test. SD: Standard deviation

Table 6: V_{80}, V_{75}, V_{70}, and V_{40} of the bladder

	Mean±SD (%) (range)				
	Treatment dose	Combined dose (half-fan mode)		Combined dose (full-fan mode)	
V_{80}	0.08±0.13 (0.00-0.41)	0.66±0.91 (0.01-3.64)	P<0.001	0.48±0.78 (0.00-3.20)	P<0.001
V_{75}	8.15±3.80 (3.34-18.14)	8.74±4.01 (3.58-19.27)	P<0.001	8.58±3.97 (3.49-19.01)	P<0.001
V_{70}	11.07±4.89 (4.44-23.90)	11.47±5.03 (4.64-24.64)	P<0.001	11.35±5.01 (4.58-24.43)	P<0.001
V_{40}	27.89±8.72 (12.80-46.16)	28.70±8.79 (13.34-46.89)	P<0.001	28.32±8.78 (13.06-46.65)	P<0.001

For V_{80}, V_{75}, V_{70}, and V_{40}, the significance of the difference between the two combined doses and planned treatment dose was evaluated using the Wilcoxon signed-rank test. SD: Standard deviation

Table 7: Rectal normal tissue complication probability (%) of treatment and combined dose

Patient number	Treatment dose	Combined dose (half-fan mode)	Combined dose (full-fan mode)
1	0.32	0.35	0.35
2	0.28	0.32	0.32
3	0.60	0.69	0.69
4	0.63	0.75	0.74
5	0.62	0.72	0.72
6	0.32	0.38	0.34
7	0.52	0.61	0.60
8	0.29	0.33	0.33
9	0.31	0.33	0.33
10	0.64	0.73	0.73
11	0.87	1.03	1.04
12	0.73	0.82	0.82
13	0.13	0.15	0.15
14	0.30	0.35	0.35
15	0.42	0.49	0.49
16	0.31	0.36	0.36
17	0.43	0.50	0.51
18	0.43	0.51	0.51
19	0.26	0.27	0.27
20	0.75	0.88	0.89
Mean (SD)	0.46 (0.20)	0.53 (0.24), P<0.001	0.53 (0.24), P<0.001

The significance of the difference between the two combined doses and the planned dose was evaluated using the Wilcoxon signed-rank test. SD: Standard deviation

absolute values, the absolute doses were a maximum of 0.12 and 0.23 cGy in the half-fan and full-fan modes, respectively. Hence, the CBCT dose was reproduced with high accuracy. In both modes, the MC-calculated dose tended to be lower at the measurement points on the floor side (7 and 9). This occurred because the CT couch was included in the calculation volume as the CT images involved the couch in the MC calculation. In the actual measurement, the CBCT dose was measured by placing an elliptical phantom on a carbon top plate with a width of 14.5 cm and height of 2.0 cm, which has lower X-ray absorption. The calculated MC doses at the measurement points on the ceiling side (1, 2, and 3) were also considered to be higher because the MC calibration and the measured value had different doses due to the different beam absorptions of the couches.

Organ dose and dose distribution combined with treatment dose and cone-beam computed tomography dose

According to the AAPM Task Group 180 Report, when the imaging dose exceeds 5% of the prescription dose, dose distributions, including the imaging dose and evaluation of the organ dose, are required.[16] With our proposed system, accurate and comprehensive determination of the CBCT dose is achievable.

In the half-fan mode, the average D_{50} values of the prostate, rectum, bladder, and pelvic bones were 0.80 ± 0.10 Gy, 0.84 ± 0.11 Gy, 0.88 ± 0.14 Gy, and 1.76 ± 0.27 Gy, respectively. Nelson *et al*. reported the imaging dose in a patient's body for one CBCT determined through MC simulations. In that study, the D_{50} ranges of the prostate, rectum, bladder, and pelvis in the half-fan mode were 1.19–1.79 Gy, 1.51–1.99 Gy, 1.36–2.20 Gy, and 2.93–3.96 Gy, respectively.[29] These doses were converted into 39 fractions, yielding 0.46–0.70 Gy, 0.59–0.78 Gy, 0.53–0.86 Gy, and 1.14–1.54 Gy, respectively, which are approximately consistent with or calculated doses. The D_2 values of the prostate, rectum, and bladder are not significantly different from D_{50}, and the dose increased uniformly owing to the small volume. On the other hand, for pelvic bones, the average D_{50} was 1.76 ± 0.27 Gy and the average D_2 was 3.92 ± 0.45 Gy. Ding *et al*. reported that the absorption of 125 kV X-rays is extremely high in bones – approximately

three times higher than in soft tissue.[9] This MC-calculated dose shows a similar tendency and thus is considered a reasonable result. In addition, D_{50} is smaller than D_2 because the volume with a high dose includes the pelvic bone volume. In the full-fan mode, the rectal dose increased by 25.0% on average, bladder dose decreased by 46.6%, and pelvic bone dose decreased by 25.0% for D_{50} compared to the half-fan mode. The full-fan mode was set such that the X-ray tube passed through the patient's back from a gantry angle of 292°–88°. Therefore, the decreased dose in the bladder can be attributed to the absence of radiation to the ventral side. The rectal dose increase in the full-fan mode is due to increased exposure time. The same effect was observed for the maximum pubic bone dose in the half-fan mode and the maximum coccyx dose in the full-fan mode.

The D_2 and D_{98} of the target increased by approximately 1 Gy in both modes because of the added CBCT dose. In addition, there was no significant change in the HI. The CBCT dose did not lose the uniformity of the target dose and increased by approximately 1 Gy.

Rectal V_{75}, V_{70}, V_{65}, and V_{60} showed similar results in both modes with increases of 0.08%–0.09%, 0.33%–0.34%, 0.29%, and 0.27%–0.28%, respectively. Despite the fact that the rectal dose exceeded the CBCT dose by approximately 1 Gy, the maximum increases of V_{75}, V_{70}, V_{65}, and V_{60} were 1.10%, 3.32%, 6.40%, and 9.25%, respectively, while they increased only 0.3% in average over all patients. The Radiation Therapy Oncology Group (RTOG) 0415 prostate IMRT dose constraints were 15%, 25%, 35%, and 50% for V_{75}, V_{70}, V_{65}, and V_{60}, respectively.[30] The treatment plan used in this study was designed considering the PTV–rectum as the target, so the RTOG0415 constraints were satisfied. V_{80}, V_{75}, V_{70}, and V_{40} of the bladder increased by 0.58%, 0.59%, 0.40%, and 0.81%, respectively, in the half-fan mode, and 0.40%, 0.43%, 0.28%, and 0.43%, respectively, in the full-fan mode. In the full-fan mode, the X-ray tube runs around the patient's back; therefore, the dose to the ventral side of the bladder is reduced. The V_{80}, V_{75}, V_{70}, and V_{40} values of the bladder calculated by adding the treatment and CBCT doses were 3.64%, 19.27%, 24.64%, and 46.89%, respectively, at maximum, satisfying the RTOG0415 constraints.[30] The dose increase due to the addition of the CBCT dose is slight, and it is unlikely that the rectal and bladder complication probability will be significantly increased. However, if the target margin on the rectum or bladder side is enlarged or the prescribed dose is escalated, a safer treatment plan should consider the dose increase of approximately 1 Gy from the 39 CBCT doses. Because the X-ray tube passes through almost half of the patient's body in the full-fan mode, it is necessary to use a revised approach, such as passing the tube through the ventral side of the body, to reduce the rectal dose.

Normal tissue complication probability of the rectum and bladder

The NTCP of 0.46% ± 0.20% in average with the treatment dose increased to 0.53% ± 0.24% with 39 fractions of CBCT. Maund *et al*. reported that the NTCP of the rectum in prostate IMRT was 1.9% when target margins of 4 or 5 mm were applied to the rectum and 1.3% when 3 mm margins were applied.[8] Because we used a rectal margin of 0 mm in the treatment plan, we can assume that our NTCP would be lower than that of Maund *et al*. CBCT can result in unplanned radiation exposure, potentially increasing the rectal NTCP by up to 0.07%. Chung *et al*. reported that IGRT reduced the setup margin and the incidence of RTOG Grade 2 or higher bladder disorders from 60% to 13% and rectal disorders from 80% to 13%.[2] The increase in rectal NTCP due to the implementation of CBCT is unlikely to have any clinical impact, while the benefits of CBCT are considered to be significant in reducing the complexity by improving the accuracy of location verification. However, unnecessary radiation exposure should be kept to a minimum, and exposure reduction measures, such as using a surface monitor and an ultrasonic monitor without exposure, adjusting imaging conditions, and using full-fan mode, should be applied.

Limitations

In this study, only CBCT doses using 125 kV X-rays were evaluated; however, in clinical practice, images are acquired using various techniques such as kV and MV images and MV CBCT. Furthermore, pelvic organ variations for each treatment were not considered in the evaluation of the treatment plan. To perform more accurate dose evaluations, we recommend considering other imaging doses besides CBCT and devising a method for correcting for internal organ displacement using CBCT images taken for each treatment. The combined dose was evaluated by simply adding the CBCT dose from kV X-rays and the therapeutic dose from MV X-rays. Therefore, biological effects due to the differences in radiation quality were not considered. Future work will include the creation of a dose distribution that considers relative biological effectiveness when accounting for the beam quality, evaluation of the DVH and NTCP when accounting for beam quality, and estimation of secondary cancer risk.

Conclusions

In this study, we demonstrated a method for evaluating combined dose distribution that has not yet been proposed. The constructed system calculates the CBCT dose of prostate IMRT by MC simulation and enables comprehensive evaluation of the treatment plan by adding the CBCT dose to the treatment dose. The CBCT dose of each organ calculated in our study can be used as a reference value when planning treatment, although some errors may occur depending on the patient's anatomy. The combined dose distribution revealed a slight increase of <1% in the percentage volume for each rectal and bladder dose and a 0.07% increase in the rectal NTCP.

Acknowledgment

We would like to thank Editage (www.editage.com) for English language editing.

Financial support and sponsorship

Nil.

Conflicts of interest

There are no conflicts of interest.

References

1. Dawson LA, Jaffray DA. Advances in image-guided radiation therapy. J Clin Oncol 2007;25:938-46.
2. Chung HT, Xia P, Chan LW, Park-Somers E, Roach M 3rd. Does image-guided radiotherapy improve toxicity profile in whole pelvic-treated high-risk prostate cancer? Comparison between IG-IMRT and IMRT. Int J Radiat Oncol Biol Phys 2009;73:53-60.
3. Bujold A, Craig T, Jaffray D, Dawson LA. Image-guided radiotherapy: has it influenced patient outcomes? Semin Radiat Oncol 2012;22:50-61.
4. Sveistrup J, af Rosenschöld PM, Deasy JO, Oh JH, Pommer T, Petersen PM, *et al*. Improvement in toxicity in high risk prostate cancer patients treated with image-guided intensity-modulated radiotherapy compared to 3D conformal radiotherapy without daily image guidance. Radiat Oncol 2014;9:44.
5. Perkins CL, Fox T, Elder E, Kooby DA, Staley CA 3rd, Landry J. Image-guided radiation therapy (IGRT) in gastrointestinal tumors. JOP 2006;7:372-81.
6. Murphy MJ, Balter J, Balter S, BenComo JA Jr, Das IJ, Jiang SB, *et al*. The management of imaging dose during image-guided radiotherapy: report of the AAPM Task Group 75. Med Phys 2007;34:4041-63.
7. Wen N, Guan H, Hammoud R, Pradhan D, Nurushev T, Li S, *et al*. Dose delivered from Varian's CBCT to patients receiving IMRT for prostate cancer. Phys Med Biol 2007;52:2267-76.
8. Maund IF, Benson RJ, Fairfoul J, Cook J, Huddart R, Poynter A. Image-guided radiotherapy of the prostate using daily CBCT: the feasibility and likely benefit of implementing a margin reduction. Br J Radiol 2014;87:20140459.
9. Ding GX, Duggan DM, Coffey CW. Accurate patient dosimetry of kilovoltage cone-beam CT in radiation therapy. Med Phys 2008;35:1135-44.
10. Ding GX, Coffey CW. Radiation dose from kilovoltage cone beam computed tomography in an image-guided radiotherapy procedure. Int J Radiat Oncol Biol Phys 2009;73:610-7.
11. Ding GX, Munro P, Pawlowski J, Malcolm A, Coffey CW. Reducing radiation exposure to patients from kV-CBCT imaging. Radiother Oncol 2010;97:585-92.
12. Ding GX, Munro P. Radiation exposure to patients from image guidance procedures and techniques to reduce the imaging dose. Radiother Oncol 2013;108:91-8.
13. Abuhaimed A, Martin CJ, Sankaralingam M. A Monte Carlo study of organ and effective doses of cone beam computed tomography (CBCT) scans in radiotherapy. J Radiol Prot 2018;38:61-80.
14. Grelewicz Z, Wiersma RD. Combined MV + kV inverse treatment planning for optimal kV dose incorporation in IGRT. Phys Med Biol 2014;59:1607-21.
15. Alaei P, Spezi E, Reynolds M. Dose calculation and treatment plan optimization including imaging dose from kilovoltage cone beam computed tomography. Acta Oncol 2014;53:839-44.
16. Ding GX, Alaei P, Curran B, Flynn R, Gossman M, Mackie TR, *et al*. Image guidance doses delivered during radiotherapy: Quantification, management, and reduction: Report of the AAPM Therapy Physics Committee Task Group 180. Med Phys 2018;45:e84-e99.
17. Kawrakow I. Accurate condensed history Monte Carlo simulation of electron transport. I. EGSnrc, the new EGS4 version. Med Phys 2000;27:485-98.
18. Kawrakow I, Mainegra-Hing E, Rogers DW, Tessier F, Walters BR. The EGSnrc code system: Monte Carlo Simulation of Electron and Photon Transport National Research Council of Canada Report PIRS-701; 2011.
19. Rogers DW, Faddegon BA, Ding GX, Ma CM, We J, Mackie TR. BEAM: a Monte Carlo code to simulate radiotherapy treatment units. Med Phys 1995;22:503-24.
20. Rogers DWO, Walters B, Kawrakow I. BEAMnrc User's Manual National Research Council of Canada Report PIRS-0509 (A) Rev L; 2018.
21. Walters B, Kawrakow I, Rogers DW. DOSXYZnrc User's Manual National Research Council of Canada Report PIRS-794 Rev B; 2018.
22. Ma CM, Coffey CW, DeWerd LA, Liu C, Nath R, Seltzer SM, *et al*. AAPM protocol for 40-300 kV x-ray beam dosimetry in radiotherapy and radiobiology. Med Phys 2001;28:868-93.
23. ICRU. Prescribing, recording, and reporting photon-beam intensity-modulated radiation threapy (IMRT). ICRU Report 83. J ICRU 2010;10:1-106.
24. Kutcher GJ, Burman C, Brewster L, Goitein M, Mohan R. Histogram reduction method for calculating complication probabilities for three-dimensional treatment planning evaluations. Int J Radiat Oncol Biol Phys 1991;21:137-46.
25. Kutcher GJ, Burman C. Calculation of complication probability factors for non-uniform normal tissue irradiation: The effective volume method. Int J Radiat Oncol Biol Phys 1989;16:1623-30.
26. Burman C, Kutcher GJ, Emami B, Goitein M. Fitting of normal tissue tolerance data to an analytic function. Int J Radiat Oncol Biol Phys 1991;21:123-35.
27. Michalski JM, Gay H, Jackson A, Tucker SL, Deasy JO. Radiation dose-volume effects in radiation-induced rectal injury. Int J Radiat Oncol Biol Phys 2010;76:S123-9.
28. Hioki K, Araki F, Ohno T, Nakaguchi Y, Tomiyama Y. Absorbed dose measurements for kV-cone beam computed tomography in image-guided radiation therapy. Phys Med Biol 2014;59:7297-313.
29. Nelson AP, Ding GX. An alternative approach to account for patient organ doses from imaging guidance procedures. Radiother Oncol 2014;112:112-8.
30. Buckey CR, Swanson GP, Stathakis S, Papanikolaou N. Optimizing prostate intensity-modulated radiation therapy (IMRT): do stricter constraints produce better dosimetric results? Eur J Clin Med Oncol 2010;2:139-44.